NANO LETTERS

pubs.acs.org/NanoLett

Letter

Rapid Joule-Heating Synthesis for Manufacturing High-Entropy Oxides as Efficient Electrocatalysts

Han Wu, Qi Lu, Yajing Li, Jiajun Wang, Yingbo Li, Rui Jiang, Jinfeng Zhang, Xuerong Zheng, Xiaopeng Han,* Naiqin Zhao, Jiajun Li, Yida Deng,* and Wenbin Hu

Cite This: *Nano Lett.* 2022, 22, 6492−6500

Read Online

ACCESS | Metrics & More | Article Recommendations | Supporting Information

ABSTRACT: High-entropy oxide (HEO) including multiple principal elements possesses great potential for various fields such as basic physics, mechanical properties, energy storage, and catalysis. However, the synthesis method of high-entropy compounds through the traditional heating approach is not conducive to the rapid properties screening, and the current elemental combinations of HEO are also highly limited. Herein, we report a rapid synthesis method for HEO through the Joule-heating of nickel foil with dozens of seconds. High-entropy rocksalt oxides (HERSO) with the new elemental combination, high-entropy spinel oxides (HESO), and high-entropy perovskite oxide (HEPO) have been synthesized through the Joule-heating. The synthesized HERSO with new elemental combinations proves to be a great promotion of OER activity due to the synergy of multiple components and the continuous electronic structure experimentally and theoretically. The demonstrated synthesis approach and the new component combination of HERSO provide a broad platform for the development of high-entropy materials and catalysts.

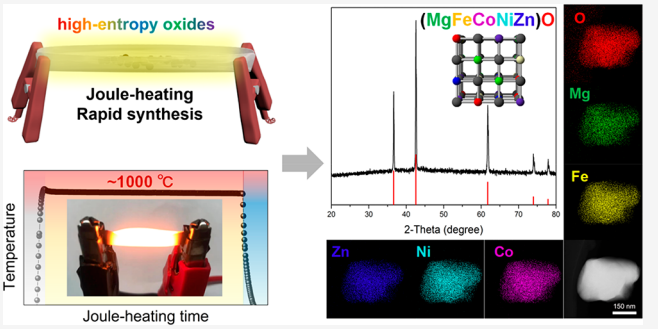

KEYWORDS: *Joule-heating, high-entropy oxide, rocksalt structure, oxygen evolution reaction*

High-entropy oxide (HEO) as an emerging class of materials composed of multiple principal metallic elements exhibits promising development potential in some significant fields including basic physics,[1−4] mechanical properties,[5−7] energy storage,[8−10] and catalysis.[11−13] Compared with the traditional doping strategy based on less-components, the mixed components of HEOs sometimes cause extra properties while averaging the properties of each principal metallic element. For instance, Ceder et al. reported the improvement of the capacity of lithium storage for HEO,[8] and Hu et al. reported superior stability for catalytic methane combustion on HEO.[13] Since the unique properties of HEOs benefit from the interaction and entropy promotion of the different combinations between multiple principal elements, exploring the new elemental combinations of HEOs through rapid high-throughput synthetic technology is necessary.

However, the synthesis method of HEOs previously reported is mainly based on the heating treatment in muffle furnaces, which requires a long time of heating, heating preservation, and cooling.[14−16] This synthesis approach is not conducive to the high-throughput screening for synthesis parameters and component combinations of HEOs. In addition, the elemental combinations in HEOs are highly limited at present such as high-entropy rocksalt oxides (HERSO) in which the studies are only limited to this elemental combination of MgCoNiCuZn because it is difficult to dissolve many other elements with different properties into the same oxide structure.[1,17−20] For instance, the large difference in ionic radius leads to the high difficulty in the formation of single-phase HEOs due to the ionic size effect in crystal, and the phase transition competition of different structures at high-temperature also leads to the difficulty increases in the formation of single-phase HEOs such as the phase transition competition of rocksalt structure and spinel structure.[21,22] Therefore, developing a new rapid and controllable synthesis strategy based on the concept of shortening the heating treatment time greatly is highly desirable, and meanwhile broadening the elemental combination of HEOs can greatly stimulate the compositional advantages of high-entropy materials.

Here, we present a new synthesis approach of Joule-heating based on nickel foil for the rapid and high-throughput synthesis of HEOs. In just dozens of seconds, the Joule-heating of nickel foil makes the precursor thermally decompose and meanwhile causes the formation of HEOs. Through the utilization of the Joule-heating technology and synthetic control of precursor, we

Received: March 24, 2022
Revised: August 7, 2022
Published: August 11, 2022

https://doi.org/10.1021/acs.nanolett.2c01147
Nano Lett. 2022, 22, 6492−6500

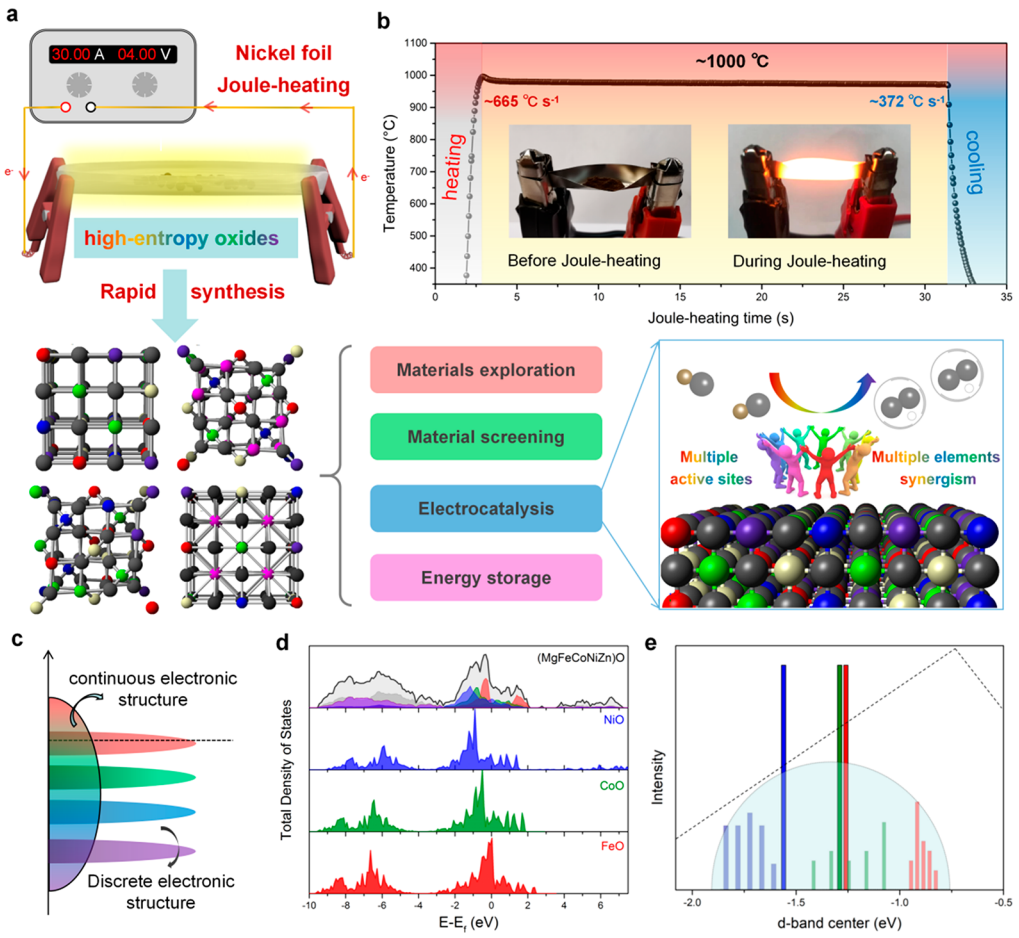

Figure 1. (a) Schematic diagram of the preparation of high entropy oxide with different structure systems by Joule heating of nickel foil for various studies as well as catalytic application. Gray balls represent oxygen, and the balls with other colors represent different metal elements. (b) The temperature curve of nickel foil during Joule-heating (insert pattern: the picture of Joule-heating). Schematic diagram of multiple active sites and synergistic catalysis on HEOs. (c) Schematic diagram of density of states (DOS) for different unary materials and high-entropy materials. (d) Total and partial density of states for the synthesized (MgFeCoNiZn)O, FeO, CoO, and NiO. (e) The statistics of d-band centers in different metal sites of (MgFeCoNiZn)O including Fe, Co, Ni, and the d-band center of unary oxides (FeO, CoO, and NiO).

synthesized a HERSO with a new combination (MgFeCoNiZn)O, in which Fe^{2+} is introduced into the rocksalt structure. In addition, the successful synthesis of other HEOs including HERSO (MgMnCoNiZn)O, HESO $(MgMnCoNiZn)Fe_2O_4$, as well as $(CrMnFeCoNi)_3O_{4-x}$, HEPO $La(CrMnFeCoNi)O_{3-x}$ indicates the synthetic universality of Joule-heating based on nickel foil for HEOs. The synthesized HERSO (MgFeCoNiZn)O exhibits great OER activity (300 mV at 10 mA cm^{-2}) compared with unary rocksalt oxides due to the synergy of multiple active sites and continuous electronic structure. Density functional theory (DFT) simulation proves the great OER activity of (MgFeCoNiZn)O according to the more continuous density of states (DOS) near the Fermi level and lower ΔG of rate-determining step (RDS). Moreover, DFT simulation exhibits a relatively linear relationship between the d-band center and OER activity in the rocksalt oxide system. In general, the synthesis approach of Joule-heating and the study of OER activity based on HERSO system provide a broad platform for the development of high-entropy materials and efficient electrocatalysts.

The possible reasons for using furnaces as heating instruments that take a long time are as follows. To ensure that the temperature in the furnace cavity reaches the predetermined value uniformly, it is necessary to make the heating rate low enough because the heating rate is too high to make the temperature of furnace wires and furnace cavity consistent. Therefore, to overcome the shortcomings of a long time of traditional heating treatments in muffle furnaces, we developed a new rapid heating method based on the Joule-heating of metal foil. Here, nickel foil is selected as the carrier of Joule-heating based on the following considerations. First, the metal nickel among cheap metals has the moderate conductivity, plasticity, and melting point so that nickel foil can be folded into some shapes, and reach a high temperature at not high current by Joule-heating. Second, the metallic activity of nickel rank low among metals, which would prevent many metal oxides from being reduced at high-temperature (Table S1). For instance, Hu et al. reported the synthesis of HEOs through the rapid heating of carbon nanofibers, but many metal oxides would be reduced by carbon nanofibers at high temperatures in the argon atmosphere.[22] The synthesis of HEO through the Joule-heating of nickel foil is simple and fast. The hydroxide precursor powder including various metal elements prepared by coprecipitation was placed in the folded nickel foil, and then the HEO formed through the thermal decomposition of the hydroxide precursor by the Joule-heating at a certain current in the argon atmosphere for tens of seconds (Figure 1a, Figures S1−S3). As shown in Figure 1b, the Joule-heating synthesis of nickel foil can reach

https://doi.org/10.1021/acs.nanolett.2c01147
Nano Lett. 2022, 22, 6492−6500

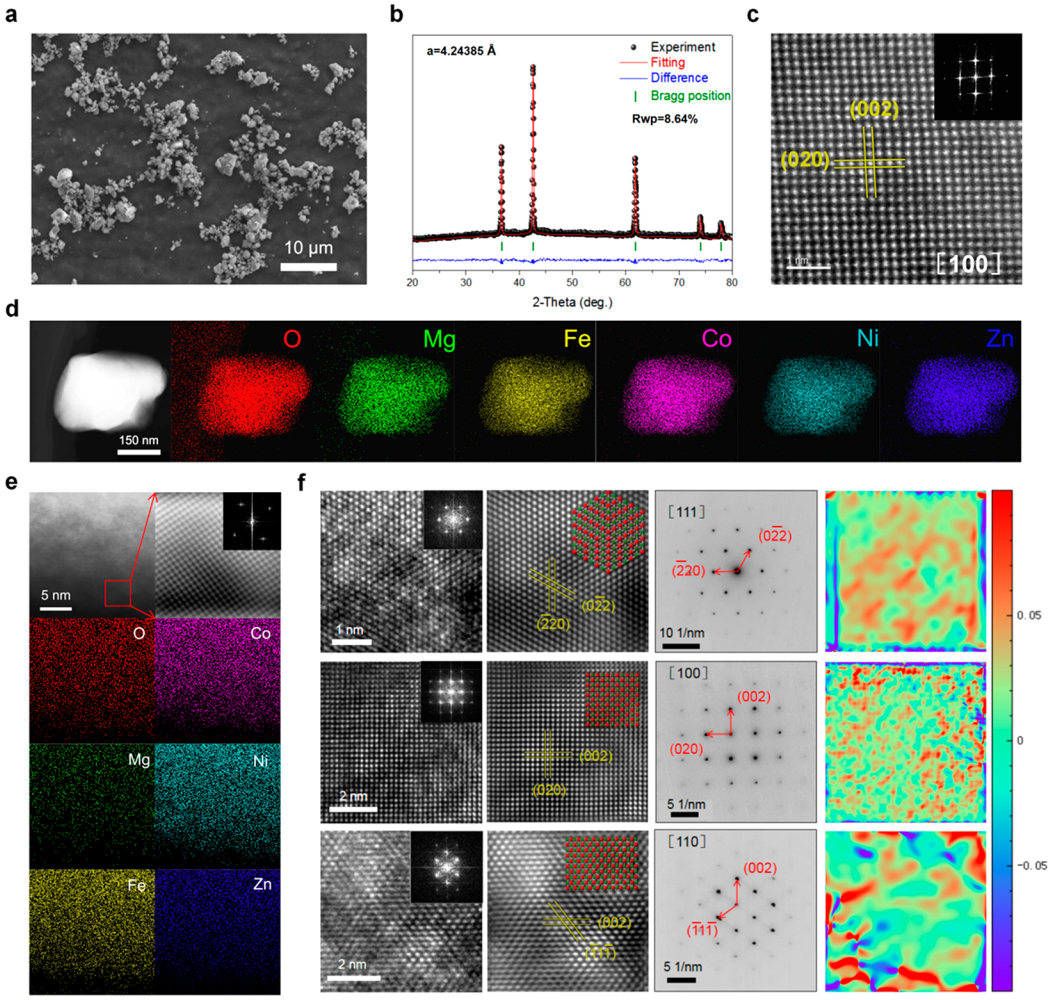

Figure 2. (a) SEM image of the synthesized (MgFeCoNiZn)O. (b) XRD pattern and refined result of (MgFeCoNiZn)O. (c) HADDF image of (MgFeCoNiZn)O (insert pattern: FFT image). (d) Elemental mapping of (MgFeCoNiZn)O. (e) Near atomic elemental mapping of (MgFeCoNiZn)O. (f) HRTEM images along [100], [111], and [110] axis and corresponding IFFT images, SAED patterns, atomic strain distribution of (MgFeCoNiZn)O.

about 1000 °C of high temperature, and a heating and cooling rate of hundreds of °C s^{-1}. Based on this Joule-heating technology, a series of HEO systems including rocksalt oxides (AO), spinel oxides (AB_2O_4 and A_3O_4), and perovskite oxides (ABO_3) are synthesized. Moreover, this synthetic approach and preparation of various HEOs also exhibit potential application in kinds of study fields such as materials exploration, materials screening, electrocatalysis, and energy storage. In particular, the HEOs synthesized via this technology exhibit high study potential in electrocatalysis such as OER due to the multiple active sites and multiple elements synergism.

As shown in Figure 1c, compared with unary materials, the high-entropy materials have a more continuous electronic structure due to the almost infinite coordination combination in high-entropy materials, which would expand the range of adsorption energy and make the adsorption more continuous to produce additional electrocatalytic properties. Therefore, relying on the Joule-heating technology, we have designed a new HERSO (MgFeCoNiZn) by introducing the Fe component with high OER activity and predicted the electronic structure and possible electrocatalytic contribution by DFT simulation.[23] Compared with unary oxide (FeO, CoO, and NiO), HERSO (MgFeCoNiZn)O shows the more continuous density of states (DOS) especially near Fermi-level, disperse d-band centers, and Bader charges (Figure 1d,e and Figures S4 and S5). The continuous electronic structure may produce some active sites with high activities according to the volcanic pattern theory.

The HERSO (MgFeCoNiZn)O have been synthesized by the Joule-heating of nickel foil at 30 A for 30 s. The temperature curve with the time exhibits a high heating rate (~665 °C s^{-1}) as well as a cooling rate (~372 °C s^{-1}), and a holding temperature of about 1000 °C (Figure 1b). The synthesized (MgFeCoNiZn)O shows the morphology of irregular-shaped particles with an average size of 700 nm from the scanning electron microscope (SEM) image and shows the rocksoalt structure without impurity according to the fitting X-ray diffraction (XRD) pattern (Figure 2a,b, Figure S6, Table S3). The high-angle annular dark-field (HAADF) image exhibits the atomic arrangement of (MgFeCoNiZn)O with rocksalt structure along [100] axis (Figure 2c). The elemental mapping at low and high magnification shows that the distribution of various elements including O, Mg, Fe, Co, Ni, and Zn are uniform at the particle scale and atomic scale (Figure 2d,e). The results above fully prove that HERSO with the new elemental combination (MgFeCoNiZn) has been successfully synthesized. Also, energy dispersive X-ray spectroscopy (EDS), X-ray

https://doi.org/10.1021/acs.nanolett.2c01147
Nano Lett. 2022, 22, 6492−6500

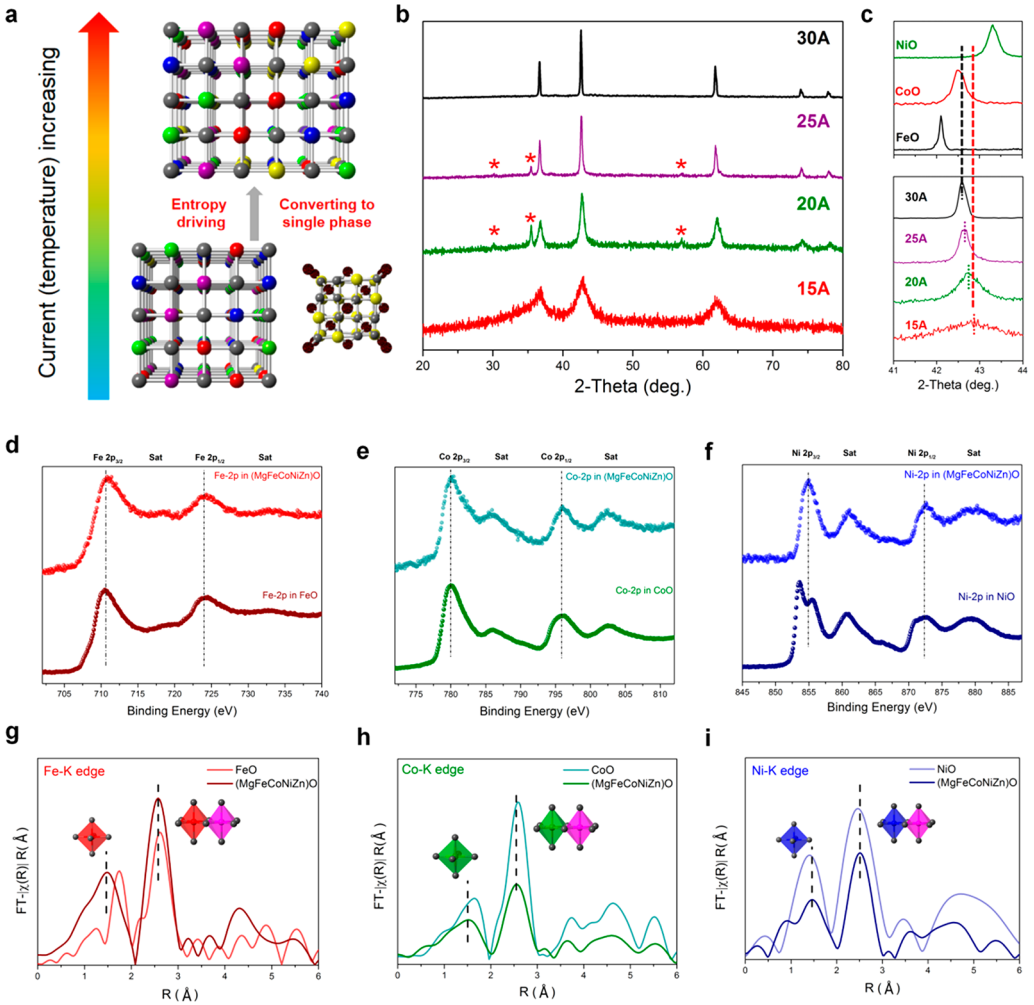

Figure 3. (a) Schematic diagram of rock salt oxide with single-phase forming driven by entropy-increasing. (b) XRD pattern of $(MgFeCoNiZn)(OH)_2$ precursor under Joule-heating with different currents. (c) Partial XRD pattern of $(MgFeCoNiZn)(OH)_2$ precursor under different Joule-heating currents compared with unary rock salt oxide (FeO, CoO, and NiO). (d–f), XPS data of Fe-3d (d), Co-3d (e), and Ni-3d (f). (g–i), Fourier-transformed k^2-weighted EXAFS data of Fe–K edge (g), Co–K edge (h), and Ni–K edge (i). (The red, green, and blue coordination polyhedrons represent the coordination structures of Fe–O, Co–O, and Ni–O. The purple coordination polyhedron represents the M-M* coordination structure of a random metal element in MgFeCoNiZn.)

photoelectron spectroscopy (XPS), and the Raman result also prove the successful synthesis of (MgFeCoNiZn)O (Figures S7–S9). To further characterize the synthesized (MgFeCoNiZn)O along the different axes, the high-resolution transmission electron microscopy (HRTEM) image, the selected area electron diffraction (SEAD) pattern, and the geometric phase analysis (GPA) are analyzed in detail. As shown in Figure 2f, the HRTEM images and corresponding IFFT images show the atomic arrangement, along the three basic axes of rocksalt structure including [100], [111], and [110] axis, which is the same as the theoretical atomic arrangement. Moreover, the SAED patterns and the crystalline planes marked along [100], [111], and [110] axes are consistent with the corresponding crystalline planes based on the HRTEM images. The atomic strain distribution pattern based on GPA shows uneven strain, in which there are many discontinuous red compressive strain regions caused by the addition of Fe^{2+} with a larger ionic radius. In addition, the synthetic process of HERSO (MgFeCoNiZn)O is analyzed and simulated in detail (Figures S10–S13).

The formation mechanism of HERSO (MgFeCoNiZn)O with a single-phase is studied in detail. Briefly, with the gradual increase of synthesis temperature, the hydroxide precursor experiences the thermal decomposition process, then transform into two structure of rocksalt structure and spinel structure, and finally transform the rocksalt structure at a higher temperature with single-phase driven by entropy (Figure 3a–c and Figure S14). According to the traditional crystallographic theory, the lattice parameters are positively related to the ionic radius. The average value of the ionic radius of the five metallic elements among (MgFeCoNiZn)O is 73.5 pm compared with 74.5 pm of Co^{2+} and 69.5 pm of Ni^{2+} indicating that the lattice parameters ($a = b = c$) of (MgFeCoNiZn)O should be slightly lower than that of CoO (Figure 3c and Table S4). Therefore, the XRD peaks of (MgFeCoNiZn)O with successful synthesis should be higher slightly than that of CoO compared with CoO and NiO. The XRD peak (200) of the sample synthesized at 15 A is in the middle of CoO and NiO, and the XRD peak (200) of the sample synthesized at 30 A is higher slightly than that of CoO indicating that Fe^{2+} with the largest ionic radius is not completely dissolved in rocksalt structure at 15 A. Compared with the previous reports, Fe^{2+} is dissolved into HERSO for the first time through the regulation of precursor in this work because Fe^{2+} is easy to be

https://doi.org/10.1021/acs.nanolett.2c01147
Nano Lett. 2022, 22, 6492–6500

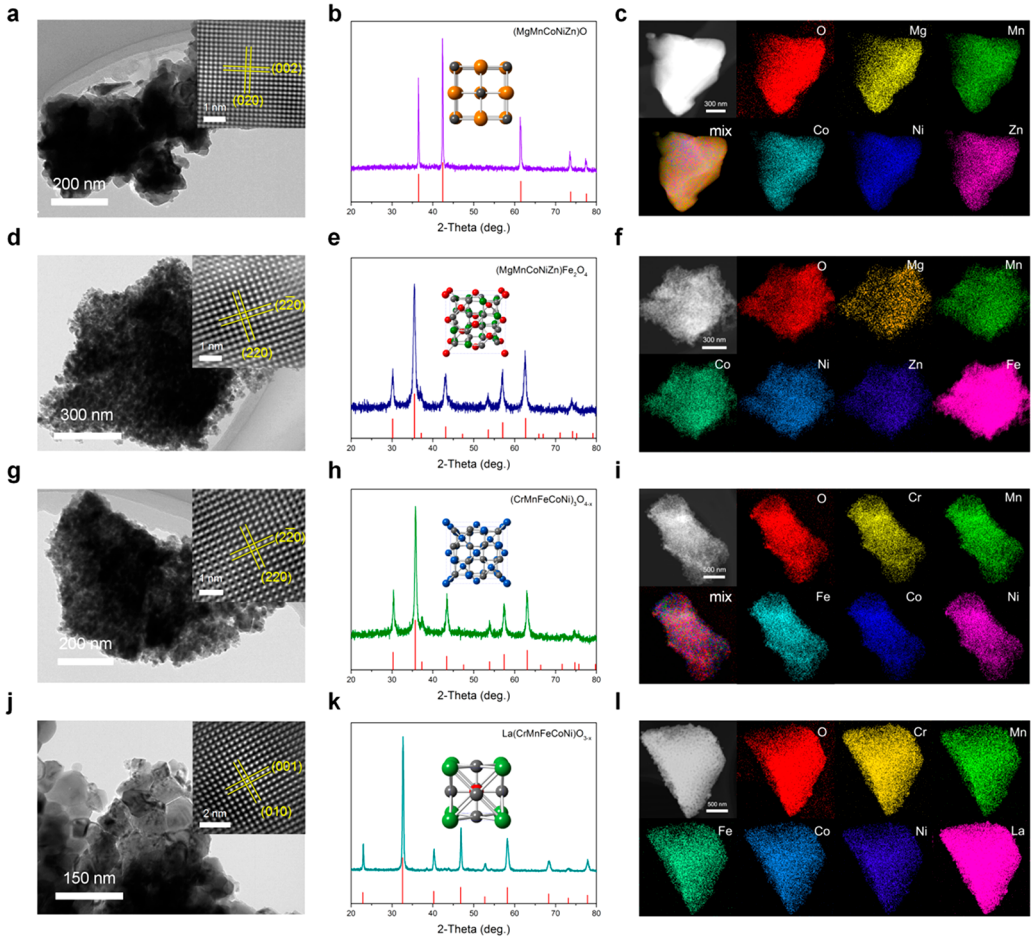

Figure 4. (a–c) TEM image (insert pattern: IFFT image) (a), XRD pattern (indexed to CoO (powder diffraction file PDF#71–1178)) (b), and elemental mapping (c) of (MgMnCoNiZn)O. (d–f) TEM image (insert pattern: IFFT image) (d), XRD pattern (indexed to $MgFe_2O_4$ (powder diffraction file PDF#88-1935)) (e), and elemental mapping (f) of $(MgMnCoNiZn)Fe_2O_4$. (g–i) TEM image (insert pattern: IFFT image) (g), XRD pattern (indexed to Fe_3O_4 (powder diffraction file PDF#75-0449)) (h), and elemental mapping (i) of $(CrMnFeCoNi)_3O_{4-x}$. (j–l) TEM image (insert pattern: IFFT image) (j), XRD pattern (indexed to $LaCrO_3$ (powder diffraction file PDF#75-0441)) (k), and elemental mapping (l) of $La(CrMnFeCoNi)O_{3-x}$.

oxidized and to form other structure such as spinel structure (Figures S15 and S16). XPS and Extended X-ray absorption fine structure (EXAFS) data for different metal elements, especially for the transition metal elements with multiple valences including Fe, Co, and Ni, have also proved the successful synthesis of HERSO (MgFeCoNiZn)O. The synthesized HERSO (MgFeCoNiZn)O shows similar XPS peaks to FeO, CoO, and NiO for Fe-2p, Co-2p, and Ni-2p, which indicates the similar surface oxidation states of (MgFeCoNiZn)O for Fe, Co and Ni to unary rocksalt structure (Figure 3d–f). Fourier-transformed k^2-weighted EXAFS data shows the M-O coordination and M-M* coordination for Fe, Co, and Ni in HERSO (MgFeCoNiZn)O, which is consistent with the unary rocksalt oxide of FeO, CoO, and NiO (Figure 3g–i and Figure S17). The difference in bonding length from the EXAFS data can be consistent with the XRD result. The average ionic radius of Mg, Fe, Co, Ni, and Zn in (MgFeCoNiZn)O (73.5 pm) is lower than that of Fe^{2+} (78 pm) and Co^{2+} (74.5 pm) and is higher than Ni^{2+}, confirmed by the XRD data. Correspondingly, the bonding length of Fe–O, Fe-M*, Co–O, and Co-M* in (MgFeCoNiZn)O is lower than that in unary FeO and CoO, and the bonding length of Ni–O and Ni-M* in (MgFeCoNiZn)O is lower than that in unary FeO (Figure 3g–i). In addition to the synthesis of (MgFeCoNiZn)O, other rock salt oxides have been synthesized and studied by Joule-heating, demonstrating the structural stability of different elemental combinations (Figures S18 and S19).

The HEOs with other components and structures have been synthesized successfully as long as the metallic activity of high-entropy components is higher than nickel, which indicates the universality of Joule-heating (Figure 4 and Figure S20). Therefore, rapid Joule-heating based on nickel foil provides a potential synthesis approach for high-throughput synthesis of HEO with various components and structures (Figure S21). Besides (MgFeCoNiZn)O can be synthesized, HERSO (MgMnCoNiZn)O can also be synthesized through Joule-heating confirmed by the XRD pattern, elemental mapping, and near-atomic level elemental mapping, in which Mn^{2+} with higher ionic radius (82 pm) can be introduced the rocksalt structure (Figure 4a–c, Figures S22 and S23). In addition to the HERSO, high-entropy spinel oxides (HESO) with two-component types of AB_2O_4 ($(MgMnCoNiZn)Fe_2O_4$) and A_3O_4 ($(CrMnFeCoNi)_3O_{4-x}$) have been synthesized successfully via Joule-heating, confirmed by XRD patterns, TEM images, and elemental mappings at different scales (Figure 4d–i, Figure S24 and 25). Additionally, high-entropy perovskite oxide HEPO ($La(CrMnFeCoNi)O_{3-x}$) has been also synthesized by Joule-heating (Figure 4j–l, Figure S26). SEM with corresponding

https://doi.org/10.1021/acs.nanolett.2c01147
Nano Lett. 2022, 22, 6492–6500

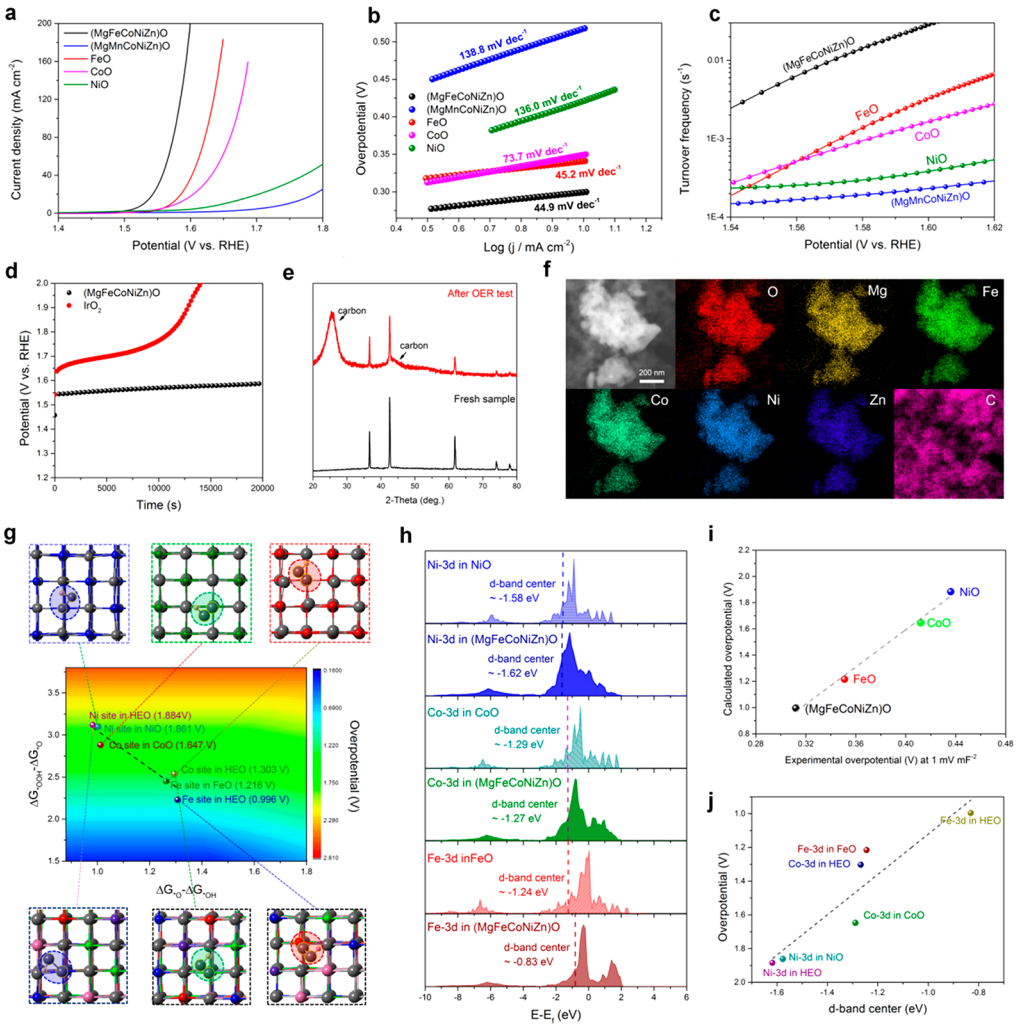

Figure 5. (a) LSV curves, (b) Tafel slope, and (c) TOF trends as a function of potential of the synthesized (MgFeCoNiZn)O, (MgMnCoNiZn), FeO, CoO, and NiO. (d) OER stability test of (MgFeCoNiZn)O and commercial IrO_2. (e) XRD pattern and (f) elemental mapping of (MgFeCoNiZn)O after OER stability test. (g) Two-dimensional map of the calculated overpotentials based on ΔG_{*OOH}-ΔG_{*O} and ΔG_{*O}-ΔG_{*OOH} at Fe site, Co site, and Ni site for (MgFeCoNiZn)O, FeO, CoO, and NiO. (h) Partial 3d density of states for (MgFeCoNiZn)O, FeO, CoO, and NiO. (i) The comparison diagram of the calculated overpotentials and experimental overpotentials for (MgFeCoNiZn)O, FeO, CoO, and NiO. (j) The pattern of the change of overpotential with d-band center for (MgFeCoNiZn)O, FeO, CoO, and NiO.

EDS data also proves that all elements in the above-synthesized HEOs basically conform to the stoichiometric ratio (Figures S27−S30). In summary, Joule-heating based on nickel foil provides a universal and rapid synthesis approach for various HEOs and less-component oxides.

Transition metal compounds, especially the oxide including the elements of Fe, Co, and Ni, have excellent OER activity confirmed by previous reports.[24,25] Therefore, the synthesized HERSO and other rocksalt oxides as OER electrocatalysts are tested and studied. The synthesized HERSO (MgFeCoNiZn)O exhibits lower overpotential (300 mV cm^{-2}) and Tafel slope (44.9 mV dec^{-1}) compared with unary oxide indicating the positive synergistic effect of elements combination for OER (Figure 5a,b and Figure S31). The synthesized HERSO (MgMnFeCoNi)O that only has one different element from (MgFeCoNiZn), shows low OER activity, which indicates the important role of Fe in OER. In addition, the OER activity of (MgFeCoNiZn)O is greatly higher than commercial IrO_2 (Figure S32). In addition, TOFs at different potentials and LSV with ECSA corrected show the better intrinsic OER activity of (MgFeCoNiZn)O (Figure 5c, Figures S33−S35). The electrochemical impedance spectroscopy (EIS) data also prove the lowest charge transfer resistance of (MgFeCoNiZn)O compared with other samples (Figure S36). The excellent OER activity of (MgFeCoNiZn)O comes from the elements of Fe, Co, and Ni as active sites and the synergy and promotion of overall metal elements (Figure S37). On the contrary, binary rocksalt oxides (CoNi)O do not show the positive OER synergy but show the average effect of CoO and NiO (Figure S38). (MgFeCoNiZn)O shows good OER stability compared with commercial IrO_2 and still remains the rocksalt structure with single-phase and uniform elemental distribution after the OER stability test (Figure 5d−f, Figure S39). In summary, (MgFeCoNiZn)O exhibits excellent OER performance compared with other samples, and multicomponents rocksalt oxides as well as HEOs reported (Table S5, Table S7).

DFT simulation is used to analyze the OER intermediate process for different unary rocksalt oxides as well as HERSO and to prove the prediction above. The adsorption energies of intermediates including *OH, *O, and *OOH, at Fe, Co, and Ni active sites are calculated for (MgFeCoNiZn)O, FeO, CoO, and NiO (Figures S40−S43, and Table S6). As shown in Figure 5g,

https://doi.org/10.1021/acs.nanolett.2c01147
Nano Lett. 2022, 22, 6492−6500

the OER activity of the Fe site and Co site as highly active sites in HERSO (MgFeCoNiZn)O increase, and the OER activity of the Ni site as relatively low active in HERSO (MgFeCoNiZn)O decreases so that the overall OER activity of (MgFeCoNiZn)O increases compared to unary FeO, CoO, and NiO. The d-band of electrocatalysts is closely related to the electrocatalytic activity. As shown in Figure 5h, the DOS of the 3d-band shifts toward the Fermi level from NiO to CoO to FeO, and the high DOS near the Fermi level is conducive to the charge transfer of electrocatalytic OER indicating the higher activity of Fe^{2+}, which is consistent with the experiment. Also, the d-band center of FeO, CoO, and NiO exhibit a similar regular phenomenon above that the d-band center of FeO, CoO, and NiO shift positively from NiO to CoO to FeO. In particular, the d-band center of Fe, Co in (MgFeCoNiZn)O shift positively compared with unary FeO and CoO while the d-band center of Ni in (MgFeCoNiZn)O shifts negatively compared with NiO. According to the above prediction, the positive shift and expansion of the d-band center may make the active sites move toward the apex of the volcanic curve, indicating the increase of OER activity in (MgFeCoNiZn)O. Moreover, there is a linear trend that the increase of active site activity in (MgFeCoNiZn)O is due to the decrease of ΔG_{*OOH}-ΔG_{*O} and increase of ΔG_{*O}-ΔG_{*OH} indicating the more continuity of intermediate adsorption in HERSO (MgFeCoNiZn), which is consistent with the analysis of DOS. The theoretical overpotentials based on the RDS of DFT simulation for (MgFeCoNiZn)O, FeO, CoO, and NiO exhibit a great linear relationship with the experimental overpotentials based on the LSV with ECAS corrected, indicating the unity of theory and experiments (Figure 5i). Additionally, the d-band centers of different samples have a relatively linear relationship with theoretical overpotentials that the OER activities increase with the increase of the d-band center in the rocksalt oxides system (Figure 5j). In summary, relying on the DFT simulation, the relationship between components and activity in HERSO can be established and can be consistent with the experiments to a certain degree.

In this work, we develop a new synthesis approach of Joule-heating based on nickel foil for the rapid synthesis of HEOs. This technology of Joule-heating provides a very fast synthesis process for only tens of seconds through the fast thermal decomposition precursor inside nickel foil. The HERSO with a new component combination (MgFeCoNiZn)O can be synthesized rapidly through this technology of Joule-heating and the regulation of precursor. Various characterizations prove the successful synthesis of HERSO (MgFeCoNiZn)O, which requires high temperature to overcome the effect of phase-transition caused spinel phase through the promotion of entropy at high temperature. The technology of Joule-heating also exhibits the synthetic university for other HEOs including HERSO ((MgMnCoNiZn)O), HESO (AB_2O_4 (MgMnCoNiZn)Fe_2O_4, and A_3O_4 $(CrMnFeCoNi)_3O_{4-x}$), HEPO ($La(CrMnFeCoNi)O_{3-x}$). The synthesized HERSO (MgFeCoNiZn)O shows great OER activity compared with unary rocksalt oxides and commercial IrO_2, due to the multiple active sites and the synergy between different elements. Moreover, the DFT simulation of (MgFeCoNiZn)O exhibits more continuous DOS near the Fermi level and lower ΔG of RDS compared with other samples indicating better OER activity of (MgFeCoNiZn)O which is consistent with experiments. In addition, there is a trend that OER activity increase with the increase of the d-band center in this system. In general, the technology of Joule-heating based on nickel foil demonstrates high potential in the rapid and high-throughput synthesis of HEOs and multiple-component oxides.

■ ASSOCIATED CONTENT

Supporting Information

The Supporting Information is available free of charge at https://pubs.acs.org/doi/10.1021/acs.nanolett.2c01147.

Additional details including the detailed experimental method, photographs for Joule-heating, temperature simulation of Joule-heating, the characterizations of a series of samples (XRD patterns, SEM images, TEM images, size distribution, wavelet transform, XPS, Raman, EDS, elemental mappings), schematic diagram of high-throughout fast synthesis, electrochemical OER data, DFT simulation data, and some tables (metal active order, parameters of temperature simulation, XRD refinement parameters, ionic radius, electrochemical OER data, the change of Gibbs free energy of each pathway on OER, the OER performance of (MgFeCoNiZn)O compared with reports) (PDF)

Movie of in situ observation of high-entropy oxide synthesis by Joule-heating of nickel foil (MP4)

■ AUTHOR INFORMATION

Corresponding Authors

Xiaopeng Han − *School of Materials Science and Engineering, Tianjin Key Laboratory of Composite and Functional Materials, Key Laboratory of Advanced Ceramics and Machining Technology, (Ministry of Education), Tianjin University, Tianjin 300350, P.R. China;* orcid.org/0000-0002-7557-7133; Email: xphan@tju.edu.cn

Yida Deng − *School of Materials Science and Engineering, Tianjin Key Laboratory of Composite and Functional Materials, Key Laboratory of Advanced Ceramics and Machining Technology, (Ministry of Education), Tianjin University, Tianjin 300350, P.R. China; State Key Laboratory of Marine Resource Utilization in South China Sea, School of Materials Science and Engineering, Hainan University, Haikou 570228, P.R. China;* orcid.org/0000-0002-8890-552X; Email: yida.deng@tju.edu.cn

Authors

Han Wu − *School of Materials Science and Engineering, Tianjin Key Laboratory of Composite and Functional Materials, Key Laboratory of Advanced Ceramics and Machining Technology, (Ministry of Education), Tianjin University, Tianjin 300350, P.R. China*

Qi Lu − *School of Materials Science and Engineering, Tianjin Key Laboratory of Composite and Functional Materials, Key Laboratory of Advanced Ceramics and Machining Technology, (Ministry of Education), Tianjin University, Tianjin 300350, P.R. China*

Yajing Li − *School of Materials Science and Engineering, Tianjin Key Laboratory of Composite and Functional Materials, Key Laboratory of Advanced Ceramics and Machining Technology, (Ministry of Education), Tianjin University, Tianjin 300350, P.R. China*

Jiajun Wang − *School of Materials Science and Engineering, Tianjin Key Laboratory of Composite and Functional Materials, Key Laboratory of Advanced Ceramics and Machining Technology, (Ministry of Education), Tianjin University, Tianjin 300350, P.R. China; Joint School of*

https://doi.org/10.1021/acs.nanolett.2c01147
Nano Lett. 2022, 22, 6492−6500

National University of Singapore and Tianjin University International Campus of Tianjin University, Binhai New City, Fuzhou 350207, P.R. China; orcid.org/0000-0001-9524-7310

Yingbo Li − *School of Materials Science and Engineering, Tianjin Key Laboratory of Composite and Functional Materials, Key Laboratory of Advanced Ceramics and Machining Technology, (Ministry of Education), Tianjin University, Tianjin 300350, P.R. China*

Rui Jiang − *School of Materials Science and Engineering, Tianjin Key Laboratory of Composite and Functional Materials, Key Laboratory of Advanced Ceramics and Machining Technology, (Ministry of Education), Tianjin University, Tianjin 300350, P.R. China*

Jinfeng Zhang − *School of Materials Science and Engineering, Tianjin Key Laboratory of Composite and Functional Materials, Key Laboratory of Advanced Ceramics and Machining Technology, (Ministry of Education), Tianjin University, Tianjin 300350, P.R. China*

Xuerong Zheng − *School of Materials Science and Engineering, Tianjin Key Laboratory of Composite and Functional Materials, Key Laboratory of Advanced Ceramics and Machining Technology, (Ministry of Education), Tianjin University, Tianjin 300350, P.R. China; State Key Laboratory of Marine Resource Utilization in South China Sea, School of Materials Science and Engineering, Hainan University, Haikou 570228, P.R. China;* orcid.org/0000-0002-0161-4077

Naiqin Zhao − *School of Materials Science and Engineering, Tianjin Key Laboratory of Composite and Functional Materials, Key Laboratory of Advanced Ceramics and Machining Technology, (Ministry of Education), Tianjin University, Tianjin 300350, P.R. China*

Jiajun Li − *School of Materials Science and Engineering, Tianjin Key Laboratory of Composite and Functional Materials, Key Laboratory of Advanced Ceramics and Machining Technology, (Ministry of Education), Tianjin University, Tianjin 300350, P.R. China*

Wenbin Hu − *School of Materials Science and Engineering, Tianjin Key Laboratory of Composite and Functional Materials, Key Laboratory of Advanced Ceramics and Machining Technology, (Ministry of Education), Tianjin University, Tianjin 300350, P.R. China; Joint School of National University of Singapore and Tianjin University International Campus of Tianjin University, Binhai New City, Fuzhou 350207, P.R. China*

Complete contact information is available at: https://pubs.acs.org/10.1021/acs.nanolett.2c01147

Author Contributions

H.W. with Y.D.D. and X.P.H. designed this project. H.W. with Q.L. and Y.J.L. prepared the samples. H.W. characterized the samples including XRD, TEM, SEM, XPS, and XAS. H.W. with Q.L. carried out the OER test. H.W. with N.Q.Z. and J.J.L. carried out the temperature simulation and DFT simulation. H.W. with J.J.W, J.F.Z, Y.B.Y., and X.R.Z. analyzed the experimental data and discussed the results. H.W. wrote this manuscript. All authors reviewed and contributed to the final manuscript.

Funding

This work was supported by the National Natural Science Foundation of China (Nos. 51571151, 51701139, 51671143, and U1601216).

Notes

The authors declare no competing financial interest.

■ ACKNOWLEDGMENTS

The work was supported at National Supercomputer Center in Tianjin, and the calculations were performed on TianHe-1(A). The work was supported by Singapore Synchrotron Light Source at National University of Singapore.

■ REFERENCES

(1) Rost, C. M.; Sachet, E.; Borman, T.; Moballegh, A.; Dickey, E. C.; Hou, D.; Jones, J. L.; Curtarolo, S.; Maria, J. P. Entropy-stabilized oxides. *Nat. Commun.* **2015**, *6*, 8485.

(2) Kozelj, P.; Vrtnik, S.; Jelen, A.; Jazbec, S.; Jaglicic, Z.; Maiti, S.; Feuerbacher, M.; Steurer, W.; Dolinsek, J. Discovery of a superconducting high-entropy alloy. *Phys. Rev. Lett.* **2014**, *113*, 107001.

(3) Lužnik, J.; Koželj, P.; Vrtnik, S.; Jelen, A.; Jagličić, Z.; Meden, A.; Feuerbacher, M.; Dolinšek, J. Complex magnetism of Ho-Dy-Y-Gd-Tb hexagonal high-entropy alloy. *Phys. Rev. B* **2015**, *92*, 224201.

(4) Schneeweiss, O.; Friák, M.; Dudová, M.; Holec, D.; Šob, M.; Kriegner, D.; Holý, V.; Beran, P.; George, E. P.; Neugebauer, J.; Dlouhý, A. Magnetic properties of the CrMnFeCoNi high-entropy alloy. *Phys. Rev. B* **2017**, *96*, No. 014437.

(5) Ding, Q.; Zhang, Y.; Chen, X.; Fu, X.; Chen, D.; Chen, S.; Gu, L.; Wei, F.; Bei, H.; Gao, Y.; Wen, M.; Li, J.; Zhang, Z.; Zhu, T.; Ritchie, R. O.; Yu, Q. Tuning element distribution, structure and properties by composition in high-entropy alloys. *Nature* **2019**, *574*, 223−7.

(6) Tong, Y.; Chen, D.; Han, B.; Wang, J.; Feng, R.; Yang, T.; Zhao, C.; Zhao, Y. L.; Guo, W.; Shimizu, Y.; Liu, C. T.; Liaw, P. K.; Inoue, K.; Nagai, Y.; Hu, A.; Kai, J. J. Outstanding tensile properties of a precipitation-strengthened FeCoNiCrTi0.2 high-entropy alloy at room and cryogenic temperatures. *Acta Mater.* **2019**, *165*, 228−40.

(7) Jung, C.; Kang, K.; Marshal, A.; Pradeep, K. G.; Seol, J.-B.; Lee, H. M.; Choi, P.-P. Effects of phase composition and elemental partitioning on soft magnetic properties of AlFeCoCrMn high entropy alloys. *Acta Mater.* **2019**, *171*, 31−9.

(8) Lun, Z.; Ouyang, B.; Kwon, D. H.; Ha, Y.; Foley, E. E.; Huang, T. Y.; Cai, Z.; Kim, H.; Balasubramanian, M.; Sun, Y.; Huang, J.; Tian, Y.; Kim, H.; McCloskey, B. D.; Yang, W.; Clement, R. J.; Ji, H.; Ceder, G. Cation-disordered rocksalt-type high-entropy cathodes for Li-ion batteries. *Nat. Mater.* **2020**, *12*, 214−221.

(9) Wang, Q.; Sarkar, A.; Wang, D.; Velasco, L.; Azmi, R.; Bhattacharya, S. S.; Bergfeldt, T.; Düvel, A.; Heitjans, P.; Brezesinski, T.; Hahn, H.; Breitung, B. Multi-anionic and -cationic compounds: new high entropy materials for advanced Li-ion batteries. *Energy Environ. Sci.* **2019**, *12*, 2433−42.

(10) Zhao, C.; Ding, F.; Lu, Y.; Chen, L.; Hu, Y. S. High-Entropy Layered Oxide Cathodes for Sodium-Ion Batteries. *Angew. Chem., Int. Ed. Engl.* **2020**, *59*, 264−9.

(11) Batchelor, T. A. A.; Pedersen, J. K.; Winther, S. H.; Castelli, I. E.; Jacobsen, K. W.; Rossmeisl, J. High-Entropy Alloys as a Discovery Platform for Electrocatalysis. *Joule* **2019**, *3*, 834−45.

(12) Lacey, S. D.; Dong, Q.; Huang, Z.; Luo, J.; Xie, H.; Lin, Z.; Kirsch, D. J.; Vattipalli, V.; Povinelli, C.; Fan, W.; Shahbazian-Yassar, R.; Wang, D.; Hu, L. Stable Multimetallic Nanoparticles for Oxygen Electrocatalysis. *Nano Lett.* **2019**, *19*, 5149−58.

(13) Yao, Y.; Huang, Z.; Xie, P.; Lacey, S. D.; Jacob, R. J.; Xie, H.; Chen, F.; Nie, A.; Pu, T.; Rehwoldt, M.; Yu, D.; Zachariah, M. R.; Wang, C.; Shahbazian-Yassar, R.; Li, J.; Hu, L. Carbothermal shock synthesis of high-entropy-alloy nanoparticles. *Science* **2018**, *359*, 1489−94.

(14) Chen, K.; Pei, X.; Tang, L.; Cheng, H.; Li, Z.; Li, C.; Zhang, X.; An, L. A five-component entropy-stabilized fluorite oxide. *Journal of the European Ceramic Society* **2018**, *38*, 4161−4.

(15) Zhao, Z.; Chen, H.; Xiang, H.; Dai, F.-Z.; Wang, X.; Xu, W.; Sun, K.; Peng, Z.; Zhou, Y. (Y0.25Yb0.25Er0.25Lu0.25)2(Zr0.5Hf0.5)2O7: A defective fluorite structured high entropy ceramic with low thermal

conductivity and close thermal expansion coefficient to Al2O3. *Journal of Materials Science & Technology* **2020**, *39*, 167−72.
(16) Dąbrowa, J.; Stygar, M.; Mikuła, A.; Knapik, A.; Mroczka, K.; Tejchman, W.; Danielewski, M.; Martin, M. Synthesis and microstructure of the (Co,Cr,Fe,Mn,Ni) 3 O 4 high entropy oxide characterized by spinel structure. *Mater. Lett.* **2018**, *216*, 32−6.
(17) Saghir, A. V.; Beidokhti, S. M.; Khaki, J. V.; Salimi, A. One-step synthesis of single-phase (Co, Mg, Ni, Cu, Zn) O High entropy oxide nanoparticles through SCS procedure: Thermodynamics and experimental evaluation. *Journal of the European Ceramic Society* **2021**, *41*, 563−79.
(18) Cardoso, A. L. F.; Perdomo, C. P. F.; Kiminami, R. H. G. A.; Gunnewiek, R. F. K. Enhancing the stabilization of nanostructured rocksalt-like high entropy oxide by Gd addition. *Mater. Lett.* **2021**, *285*, 129175.
(19) Mnasri, W.; Bérardan, D.; Tusseau-Nenez, S.; Gacoin, T.; Maurin, I.; Dragoe, N. Synthesis of (MgCoNiCuZn)O entropy-stabilized oxides using solution-based routes: influence of composition on phase stability and functional properties. *J. Mater. Chem. C* **2021**, *9*, 15121−31.
(20) Qiu, N.; Chen, H.; Yang, Z.; Sun, S.; Wang, Y.; Cui, Y. A high entropy oxide (Mg0.2Co0.2Ni0.2Cu0.2Zn0.2O) with superior lithium storage performance. *J. Alloy. Compd.* **2019**, *777*, 767−74.
(21) Zhai, S.; Rojas, J.; Ahlborg, N.; Lim, K.; Toney, M. F.; Jin, H.; Chueh, W. C.; Majumdar, A. The use of poly-cation oxides to lower the temperature of two-step thermochemical water splitting. *Energy Environ. Sci.* **2018**, *11*, 2172−8.
(22) Li, T.; Yao, Y.; Huang, Z.; Xie, P.; Liu, Z.; Yang, M.; Gao, J.; Zeng, K.; Brozena, A. H.; Pastel, G.; Jiao, M.; Dong, Q.; Dai, J.; Li, S.; Zong, H.; Chi, M.; Luo, J.; Mo, Y.; Wang, G.; Wang, C.; Shahbazian-Yassar, R.; Hu, L. Denary oxide nanoparticles as highly stable catalysts for methane combustion. *Nature Catalysis* **2021**, *4*, 62−70.
(23) Zhang, B.; Wang, L.; Cao, Z.; Kozlov, S. M.; Garcia de Arquer, F. P.; Dinh, C. T.; Li, J.; Wang, Z.; Zheng, X.; Zhang, L.; Wen, Y.; Voznyy, O.; Comin, R.; De Luna, P.; Regier, T.; Bi, W.; Alp, E. E.; Pao, C.-W.; Zheng, L.; Hu, Y.; Ji, Y.; Li, Y.; Zhang, Y.; Cavallo, L.; Peng, H.; Sargent, E. H. High-valence metals improve oxygen evolution reaction performance by modulating 3dmetal oxidation cycle energetics. *Nature Catalysis* **2020**, *3*, 985−92.
(24) Tahir, M.; Pan, L.; Idrees, F.; Zhang, X.; Wang, L.; Zou, J.-J.; Wang, Z. L. Electrocatalytic oxygen evolution reaction for energy conversion and storage: A comprehensive review. *Nano Energy* **2017**, *37*, 136−57.
(25) Yu, M.; Budiyanto, E.; Tüysüz, H. Principle of Water Electrolysis and Recent Progress of Cobalt, Nickel, and Iron-based Oxides for Oxygen Evolution Reaction. *Angew. Chem., Int. Ed.* **2021**, *61*, No. 202103824.

https://doi.org/10.1021/acs.nanolett.2c01147
Nano Lett. 2022, 22, 6492−6500